

PARAMETER BASED SCAL - ANALYSING RELATIVE PERMEABILITY FOR FULL FIELD APPLICATION

Einar Ebeltoft, Frode Lomeland, Amund Brautaset and Åsmund Haugen
Statoil ASA, Stavanger, Norway

This paper was prepared for presentation at the International Symposium of the Society of Core Analysts held in Avignon, France, 8-11 September, 2014.

ABSTRACT

A method is proposed where the flow properties from SCAL experiments are parameterized and implemented into saturation functions for full field applications. Parameterization of the flow properties facilitates analysis of end point saturations and curve shapes individually for each SCAL experiment, and storing the parameters in a SCAL database. A number of these parameterized SCAL experiments are subsequently combined to generate representative saturation functions for full field application that are consistent with wettability as well as rock properties.

The method starts by verifying each SCAL experiment by simulation followed by parameterization of the appropriate flow properties, including residual oil saturation (S_{orw} or S_{org}), end point relative permeabilities ($k_{rw}(S_{orw})$ or $k_{rg}(S_{org})$) and the shape parameters of the curves. These flow parameters are then stored in a SCAL database and interrelated with plug specific data, including experimental conditions and geo-references. Each flow parameter is analysed individually as functions of initial water saturation, porosity and permeability and supported by wettability consistent trend models. The trend models for each flow parameter have been developed based on the underlying theory of wettability, reservoir physics and observed behaviour of a large set of SCAL data from the Norwegian Continental Shelf. The trend models and application are presented in this paper.

The advantage of parameterization, using trend models and possible analogues from the database, are smooth and well defined saturation functions that are consistent with wettability. The resulting relative permeability is determined as a base case with optimistic and pessimistic bounds. These are easily implemented as saturation functions in full field reservoir simulators for sensitivity and field performance analyses. This approach is demonstrated for a real field case from the Norwegian Continental Shelf, taking the underlying theory behind trend models, rock quality and wettability into consideration.

INTRODUCTION

Relative permeability is important input for describing dynamic behaviour of fluid flow in reservoir simulators and they are required properties in the saturation equation describing multi-phase flow in porous media. These flow properties are represented as saturation functions and will significantly influence the simulated and history matched production profiles. The industry has determined these flow properties by SCAL experiments since the late 30's [1] and it is still the main approach to access saturation functions for full field applications. The design of proper SCAL programs have improved the last couple of decades as there has been significant focus on selecting and preparing representative core samples to obtain "true" wettability, performing the experiments at reservoir conditions and using live reservoir fluids. Several types of SCAL

experiments are also combined with proper rates and fluids to mimic the reservoir behaviour. Experimental equipment has improved by high precision equipment (pumps, transducers, separators, etc.) and by monitoring of *in situ* saturations. Each SCAL experiment is routinely verified by core flow simulations for verification and quality assurance, and in recent years the use of pore scale models has also been increasingly used as support to experimental data. Hence, there are numerous publications regarding how to determine and properly understand multi-phase flow in core plugs. The majority of these publications focus on determining flow properties from single core flow experiments and less is found in the literature on combining the results from several experiments to provide saturation functions for full-field application.

Nevertheless, some publications have addressed the benefits of using bulk data and studied trends between various properties. There are well-known trends between porosity and permeability. There are also clear trends between saturation end-points (S_{wi} , S_{orw} , S_{org}) and curve shapes in fluid/rock-systems at strongly wetted conditions – mainly water-wet – as the flow properties are mainly influenced by pore geometry and topology [2] However, when wettability is taken into account, the clear trends tend to vanish [3]. The effect of wettability on oil recovery and relative permeability curves have been well established during the last couple of decades and are emphasized by Hamon [3] and its references. The importance of accounting for field wettability variations was suggested by Hamon [3, 4] and also used by Ghedan *et al.* [5, 6] to give proper sets of relative permeability curves suitable for reservoir simulators. Several papers also address the importance of introducing trends between dynamic and static properties to improve dynamic flow characterization, see [5] and its references.

Trend models for relative permeability parameters have been developed based on a physical understanding of multi-phase flow in porous media and how shape and end points of the relative permeability curves should behave with respect to permeability, S_{wi} and wettability. This paper suggests a method for anchoring experimentally measured relative permeability curve shapes and end points to these trend models. In addition, a database for storage of parameterized relative permeability curves was developed. The database allows easy comparison of field specific or analogue SCAL data. We have observed that SCAL data from the Norwegian Continental Shelf (NCS) align with trends based on physics, all though some trends are more obvious than others. We observe that trends can be used to propagate bulk-data into a suitable format for saturation functions provided as a base case, with optimistic and pessimistic bounds. Using this approach elevates the uncertainty from focusing on the accuracy in each experiment to analysing the scatter of each parameter from a number of experiments.

The methodology presented here can be extended to model the Capillary Transition Zone (CTZ), in which wettability, and hence the curve shape and end-points of the relative permeability curves vary with height above oil-water contact [3-6]. This paper is based on clastic reservoir rock, but it can also be extended to other rock types such as carbonates, when sufficient bulk data is available and properly parameterized and stored in a database.

RELATIVE PERMEABILITY EXPERIMENTS AND SENSITIVITIES

The most common experiments used to determine relative permeability and residual saturations are steady state, unsteady state and single speed centrifuge. The three types of experiments provide information in different saturation ranges as indicated in Figure 1.

The *steady state* method provides two-phase relative permeabilities in a wide saturation range, but is generally not recommended as a reliable measure of residual saturation.

The *unsteady state* method provides two-phase relative permeabilities in a narrow saturation range at high saturations, and is generally not recommended as reliable measure of residual oil saturation.

The *single speed centrifuge* method provides tail-end relative permeability for the displaced phase toward its residual saturation, and is well suited for determining residual saturation.

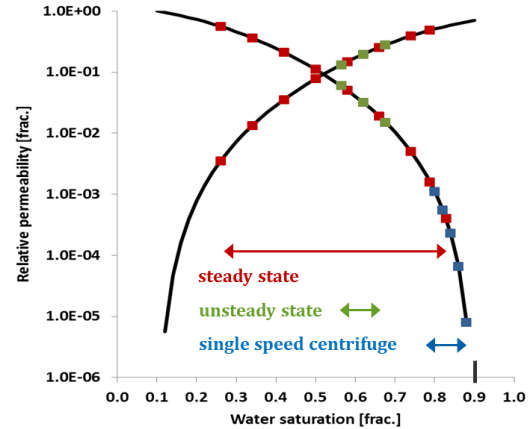


Figure 1: Relative permeability experiments and the saturation range in which they provide information

In addition to these experiments for determining relative permeability, multi-speed centrifuge is used to determine capillary pressure and wettability. This method is also well suited for determining residual saturation. In order to cover the widest possible saturation range of the relative permeability curves, it is recommended to combine these experiments when designing a SCAL program [7, 8].

LET FLOW PARAMETERS AND RELATIVE PERMEABILITY

All experiments are generally verified by Sendra core flood simulator [9] where the relative permeability curves are parameterized using the *LET* correlation [10], Eq.1-3 for oil/water.

$$k_{ro} = k_{ro}^0 \frac{(1 - S_w^*)^{L_o}}{(1 - S_w^*)^{L_o} + E_o \cdot (S_w^*)^{T_o}} \tag{Equation 1}$$

$$k_{rw} = k_{rw}^0 \frac{(S_w^*)^{L_w}}{(S_w^*)^{L_w} + E_w \cdot (1 - S_w^*)^{T_w}} \tag{Equation 2}$$

$$S_w^* = \frac{S_w - S_{wir}}{1 - S_{orw} - S_{wir}} \tag{Equation 3}$$

k_{ro}^0 is the end point relative permeability to oil at irreducible water saturation (S_{wir}) and k_{rw}^0 is the end point relative permeability to water at residual oil saturation (S_{orw}). The respective *LET* parameters for oil- and water relative permeabilities dominate different parts of the curves as illustrated in Figure 2: *L* describes the shape of the lower part of relative permeability curve, *E* describes the shape of the intermediate height of the curve and *T* describes the upper (or top) part of the curve. The *L*, *E* and *T* parameters in the *LET* correlation replace the Corey exponent, allowing smooth and flexible relative

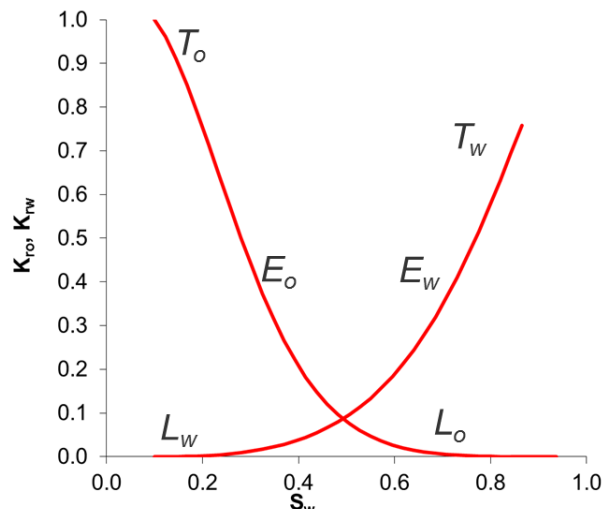


Figure 2: Dominating parts of the *LET* parameters.

permeability curves. All the individual *LET* shape parameters and end points are stored in a SCAL database with plug data, experimental conditions and geo-references (well name, plug depth, fluid viscosities at reservoir conditions, formation name, etc.).

TREND MODELS FOR LET FLOW PARAMETERS

Each flow parameter in the *LET* correlation has assigned individual *trend models* as a function of S_{wi} . The trend models have been developed based on physics and wettability considerations, and they are anchored to SCAL-data from the Norwegian Continental Shelf (NCS). The trend models were developed to create relative permeability curves and to capture the scatter normally seen in experimental data. They are consistent with wettability and physical considerations of multi-phase flow in porous media. Each trend model is calibrated to fit the field specific SCAL-data. The paper presents trend models for water-oil imbibition.

Initial water saturation, residual oil saturation

Initial water saturation (S_{wi}) defines starting point in most water-oil SCAL experiments. Wettability has been shown to be strongly affected by S_{wi} as indicated in Figure 3; lower S_{wi} tends to produce less water-wet states [11, 12]. As the S_{wi} is low, a relatively large fraction of the pore wall surface has been contacted by oil for wettability alteration towards less water-wet or even oil-wetting conditions. Low S_{wi} is typically experienced for high permeable samples. The residual oil saturations after waterflood is a function of wettability, as the minimum residual oil saturation is usually reported near to neutral-wet conditions [12-15], an example of this is shown in Figure 4 (left). The residual oil saturation is also a function of the initial oil saturation [14, 16, 17]. This is exemplified for various wettabilities by contact angles and pore scale modelling shown in Figure 4 (right). There is thus an interrelationship between S_{orw} , S_{wi} and wettability.

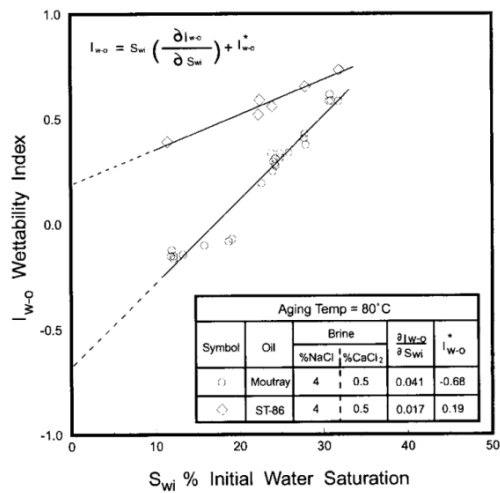


Figure 3: Amott Wettability index as function of various initial water saturations [12].

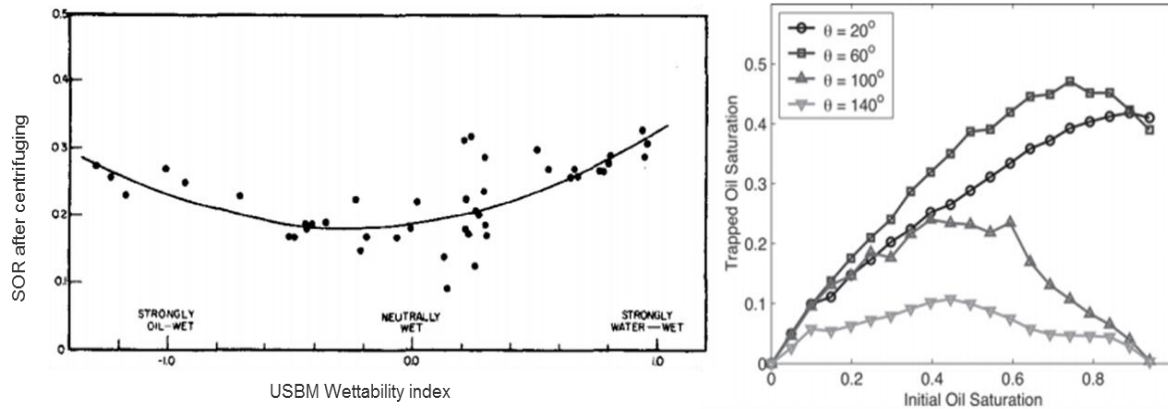


Figure 4: *Left*: Residual Oil saturation as function of USBM wettability Index from [15]. *Right*: Network modelling of trapped oil or residual oil saturation as function of initial oil saturation for different oil-water contact angles from [14].

Modified from Lomeland *et al.* we have derived the correlation between S_{wi} and S_{orw} [18].

$$S_{orw} = \frac{(A_{orw} + B_{orw} S_{wi}^{M_{orw}})(1 - S_{wi})^{L_{orw}}}{(1 - S_{wi})^{L_{orw}} + E_{orw} S_{wi}^{T_{orw}}} \quad \text{Equation 4}$$

The typical trend for this relationship is shown in Figure 5 and coincides with Figure 4 (left). The trend is consistent with increasing S_{orw} by increasing S_{wi} until a maximum is reached where S_{orw} decreases with increasing S_{wi} coinciding with Figure 4 (right) for all wettabilities. Figure 4 is hence used to exemplify the relationship between low water saturation and wettability.

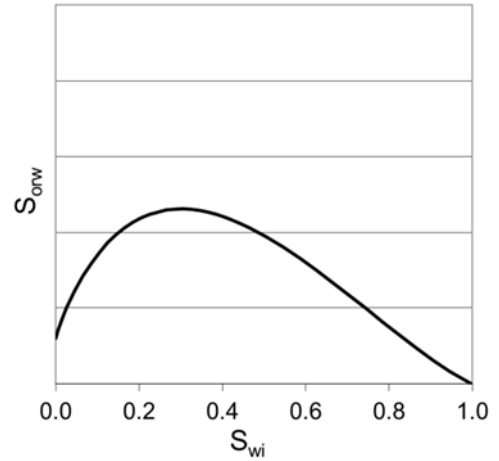


Figure 5: Typical trend model for S_{orw} versus S_{wi} by use of Equation 4.

End point water relative permeability

Relative permeability and wettability are correlated [19]. Increased water-wetness tends to result in low end-point relative permeability to water [20] and a more depressed relative permeability to water in the entire mobile saturation range. The interrelation between S_{wi} and wettability thus provides the basis for the trend model relating the end-point water relative permeability to S_{wi} , derived by Lomeland *et al* [10, 18] given by Equation 5, but here generalized with maximum parameter A_{wko} and minimum parameter C_{wko} .

$$k_{rw}^0 = C_{wko} + \frac{(A_{wko} - C_{wko}) \cdot (1 - S_{orw} - S_{wi})^{L_{wko}}}{(1 - S_{orw} - S_{wi})^{L_{wko}} + E_{wko} S_{orw}^{T_{wko}}} \quad \text{Equation 5}$$

Typical trend models for end-point relative permeability to water ($k_{rw}(S_{orw})$) as function of S_{wi} is shown in Figure 6. The model is consistent with increasing S_{wi} leading to increased water-wetness, acknowledging that more water-wet behaviour leads to lower relative permeability to water. The trend model for $k_{rw}(S_{orw})$ is closely related to the trend model for S_{orw} versus S_{wi} in Figure 5. Low S_{wi} leads to low S_{orw} , and consequently the $k_{rw}(S_{orw})$ is high. High S_{wi} also leads to low S_{orw} , however, it also leads to strongly water-wet conditions and consequently the $k_{rw}(S_{orw})$ is low.

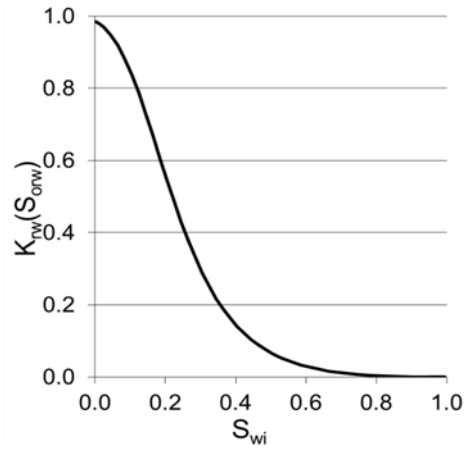


Figure 6: Typical trend models for end-point relative permeability to water as function of S_{wi} by use of Equation 5.

LET shape parameters

The shape of the relative permeability curves are captured through the *LET* parameters for oil and water. It is important that the trend models for these also reflect the change in wetting behaviour with changing S_{wi} . Figure 7 shows typical trend models for *LET* shape parameters for oil. Increasing S_{wi} leads to more water-wet behaviour and thus increased oil relative permeability, which is consistent with the trend models for L_o , E_o and T_o . Similarly, trend models for the *LET* parameters for water are shown in Figure 8. The models are consistent with increasing S_{wi} causing a more water-wet system with lower relative permeability and thus a more depressed

relative permeability shape of the water. Reversely, more oil-wet behaviour results in higher water relative permeability.

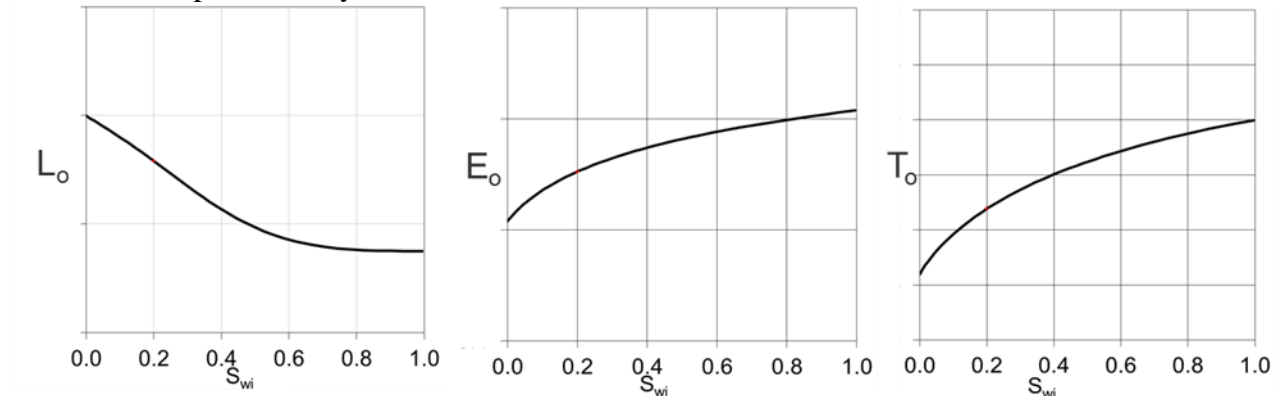


Figure 7: Typical trend model for L_o , E_o and T_o as functions of S_{wi} .

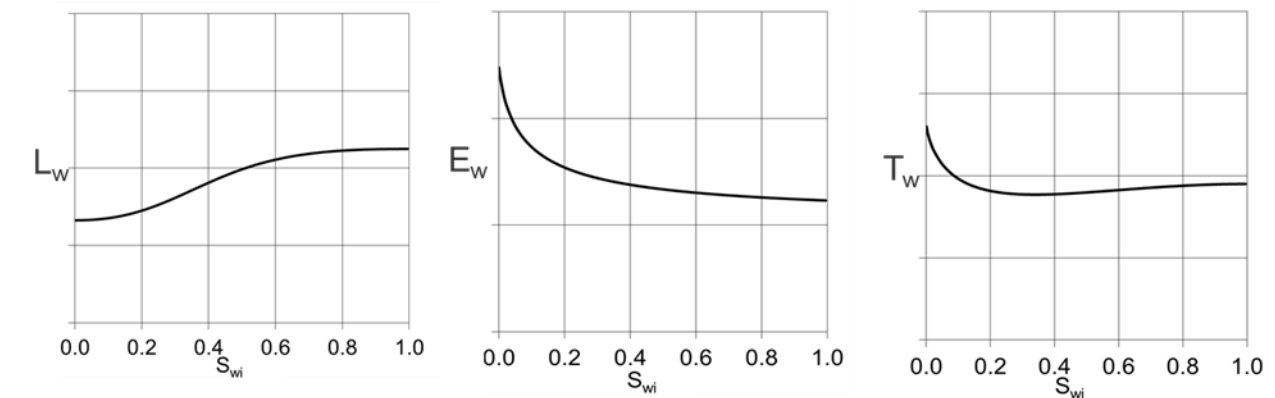


Figure 8: Typical trend model for L_w , E_w , and T_w as functions of S_{wi} .

Field-specific trend models

Wettability and relative permeability are not only functions of S_{wi} , they are also a function of chemical interactions between crude oil/brine/rock (COBR) [21-27] and the geological features of the reservoir rock, mineralogy, clay content, pore size distribution etc. It is thus necessary to calibrate the trend model to incorporate the observations made by the special core analysis measurements for the particular field in question. This is achieved by interpreting all relevant SCAL experiments and parameterizing all relative permeabilities to the LET formulation. All LET parameters are stored in a SCAL database together with plug data and geo-references (well-name, depth, formation name, etc.) Each individual trend model can then be expressed and calibrated to the field specific properties.

A SCAL program consists of several experiments, all with variations in the actual properties due to the variability within core plugs and the inherent uncertainty of experimental measurements. There will be varying S_{wi} , S_{orw} , and LET parameters within a selection of relative permeability measurements, and a method for calibrating trend models to a selection of relative permeability measurements has been developed. The individual LET flow parameters are loaded into a graphical interface overlain by the trend models shown in Figure 5-8. All trend models are given with an expected base curve visually bounded by high and low curves to capture the scatter in each flow parameter S_{orw} , $k_{rw}(S_{orw})$, L_o , E_o , T_o , L_w , E_w and T_w . Each individual trend model is then calibrated by changing the trend model inputs to better capture the field specific SCAL-data.

This is illustrated in Figure 9. The left plot shows a general trend model for S_{orw} versus S_{wi} . Plug measurements from an actual field is the blue squares and may deviate from the general trend. The right plot shows the calibrated trend models. Three models have been introduced, a base model bounded by high and low models. This captures the scatter in the SCAL data and gives a field specific trend model for S_{orw} versus S_{wi} including a span of uncertainty. Note that calibration is done by visual inspection, but based on the described trend models and field specific SCAL data. The advantage of the graphical method for calibrating the trend models are:

- Easy identification of outliers which are not representative.
- Easy determination and evaluation of the scatter in the data selection.
- Fast calibration of trend models to capture base case trend models with high and low bounds for uncertainty.

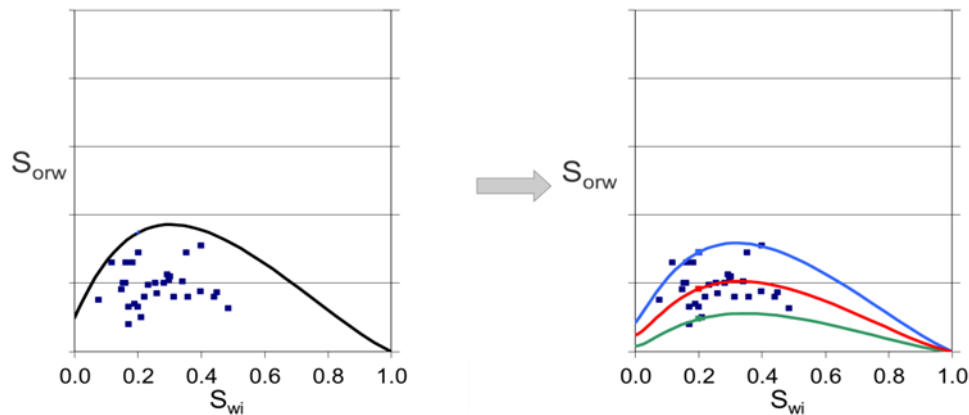


Figure 9: *Left*: Typical trend model for S_{orw} versus S_{wi} , blue squares represent plug measurements. *Right*: Three calibrated trend models are introduced; low, base and high. The trend models have been calibrated to better capture plug measurements (blue squares). Red is the expected model, bounded by high and low trends in blue and green to capture uncertainty.

This process is performed for all the flow parameters, including, S_{orw} , $k_{rw}(S_{orw})$, L_o , E_o , T_o , L_w , E_w and T_w , Figure 9-12. All trend models are given with an expected base curve bounded by high and low curves to capture the uncertainty. It should be addressed that all the standard experimental methods (steady state, unsteady state and single speed centrifuge) for waterflood relative permeability measurements have low sensitivity near S_{wi} . This implies that there is often observed more scatter in the L_w and T_o parameters, and there is in general more uncertainty associated with these two parameters and also more uncertainty in the trend models for these two parameters.

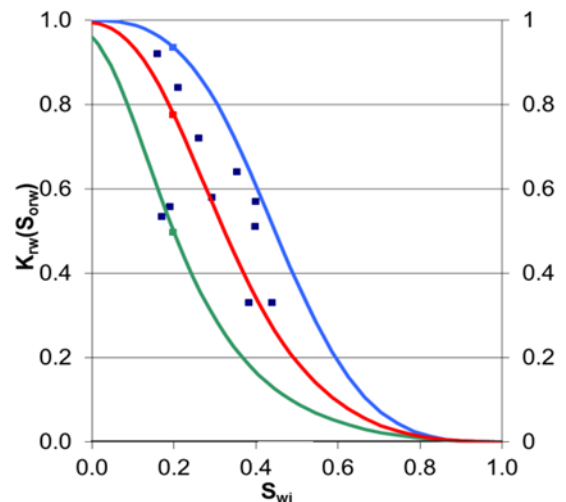


Figure 10: Calibrated trend for end point relative permeability to water, $k_{rw}(S_{orw})$, with low base and high.

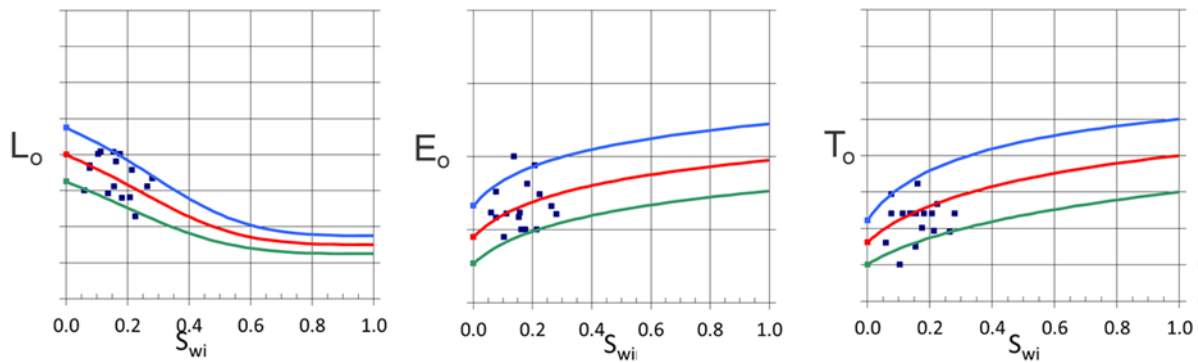


Figure 11: Calibrated trend models for L_o , E_o and T_o with low, base and high.

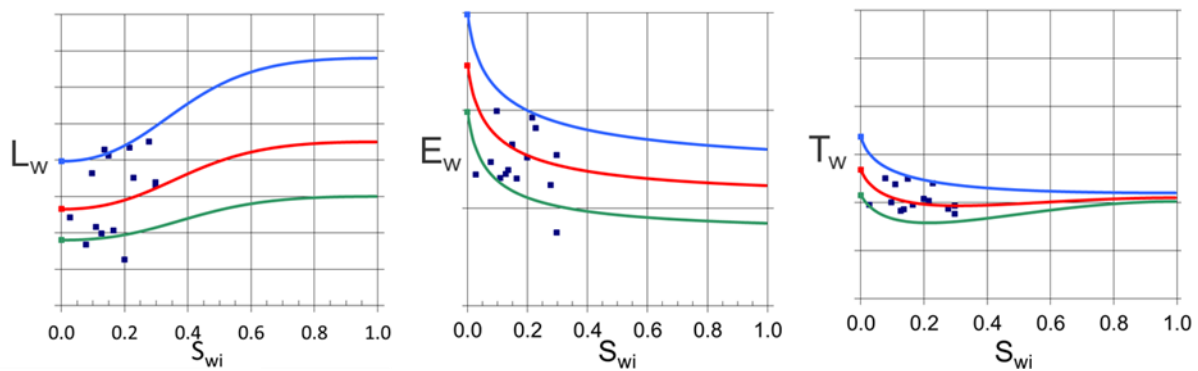


Figure 12: Calibrated trend models for L_w , E_w and T_w with low, base and high.

Generating relative permeability curves for full field simulations

When all LET parameters models have been calibrated to the field specific models (Figure 9-12), full field relative permeability curves are generated using the field specific trend models. A common way of implementing relative permeability curves in full field applications is the use of end-point saturation scaling of both relative permeability curves [28]. This introduces errors in the oil relative permeability curve shape that is not consistent with wettability. Increased S_{wi} leads to higher curvature of the oil relative permeability curve shape when end-point saturation scaling is implemented. This is inconsistent with wettability. The proposed technique to reduce the effect of end point scaling in full field simulations is to use the specific trend model to generate relative permeability over a smaller saturation interval or bin. Figure 13-16 show how 4 initial water saturations were selected for a field at the NCS. Each S_{wi} represents a saturation bin with given LET parameters which represent the oil and water relative permeability curves with optimistic and pessimistic bounds.

The example shown below has four saturation bins at $S_{wi} = [0.0 - 0.15, 0.15 - 0.25, 0.25 - 0.35, 0.35 - 1.0]$. Each bin represents a unique rock type where permeability increases with decreasing S_{wi} , i.e good quality reservoir rock is associated with the low S_{wi} , and poorer reservoir rock is associated with higher S_{wi} . Figure 13 shows the relationship between S_{wi} and absolute permeability, indicating that curve shape and end point parameters also may be correlated to permeability rather than S_{wi} in the region above the capillary transition zone.

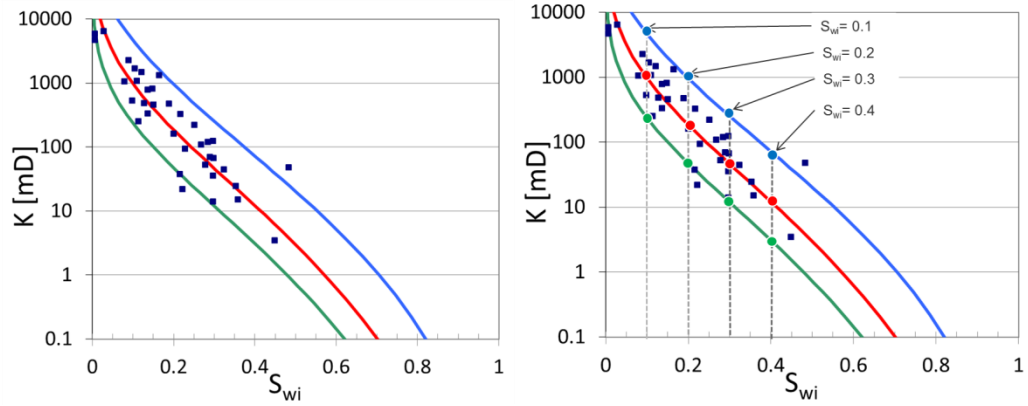


Figure 13: Relationship between S_{wi} and absolute permeability.

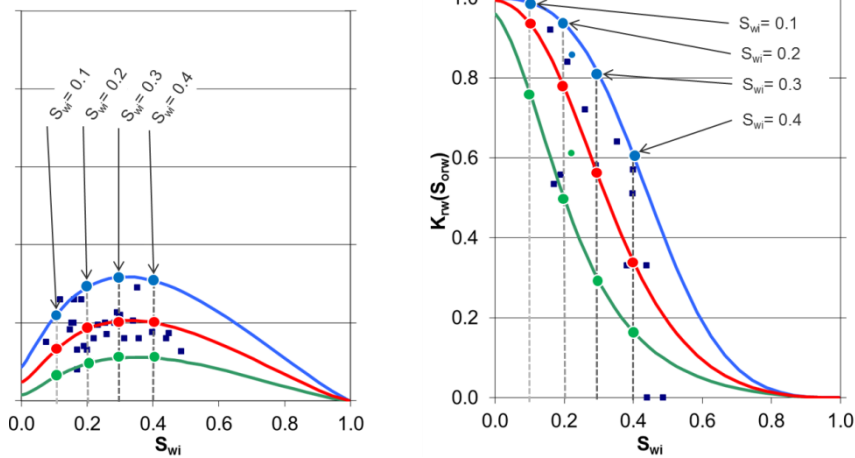


Figure 14: *Left*: Trend models for S_{orw} as function of S_{wi} with upper and lower bounds. *Right*: Trend models for endpoint relative permeability to water with upper and lower bounds. The dark blue squares are the individual values from SCAL plug experiments from Field A.

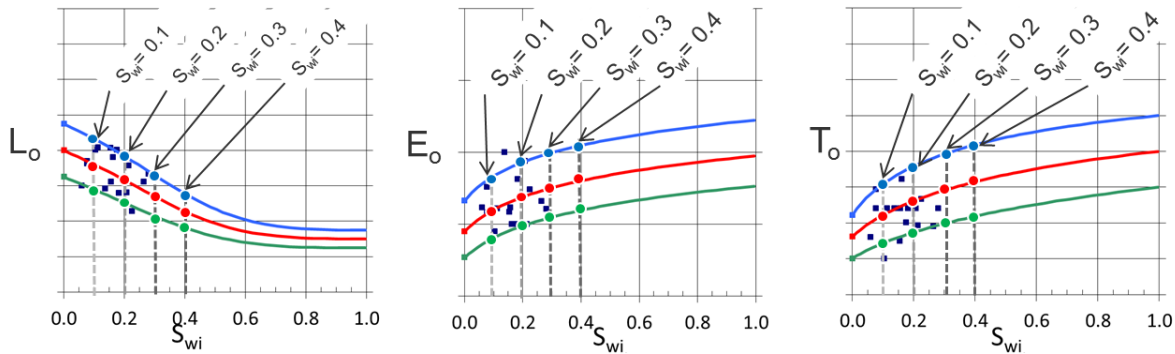


Figure 15: *Left*: Trend models for L_o as function of S_{wi} . *Middle*: Trend models for E_o as function of S_{wi} . *Right*: Trend models for T_o as function of S_{wi} . Blue squares represent values from plug experiments from Field A.

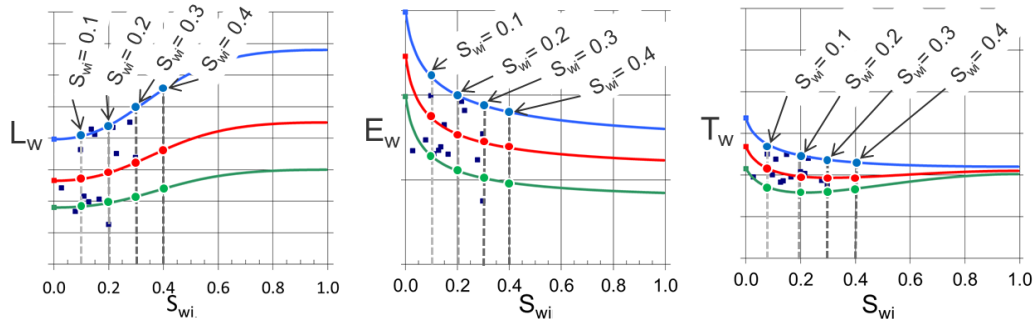


Figure 16: *Left*: Trend models for L_w as function of S_{wi} . *Middle*: Trend models for E_w as function of S_{wi} . *Right*: Trend models for T_w as function of S_{wi} . Blue squares represent values from plug experiments from Field A.

Throughout the rest of this paper we refer to S_{wi} that is established at high capillary pressure using porous plate or centrifuge, resulting in a S_{wi} that is pragmatically similar to irreducible water saturation (S_{wir}). Hence, we emphasize the reservoir region above the capillary transition zone where the production well starts by producing oil and practically no water. S_{wir} varies with absolute permeability across the reservoir, and it defines the lowest water saturation and it is anchoring the relative permeability curves. The resulting relative permeability curves for *the first bin* with base, optimistic and pessimistic curves are shown in Figure 17 (left). The resulting *base case* relative permeabilities for all 4 bins are shown in Figure 17 (right). Note that both shape and end points of the relative permeability changes as S_{wi} increases. The advantage of this method is relative permeabilities that are easily implemented in full field simulations, and they are consistent with wettability and permeability in a large saturation range. The analysis of each individual parameter provides a good measure of the uncertainty and scatter in experimental data from SCAL.

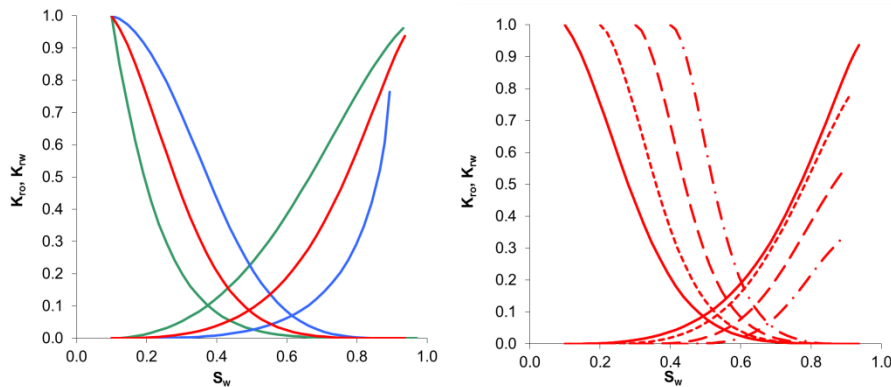


Figure 17: *Left*: Relative permeability for highest permeability rock type, i.e. the lowest S_{wi} with base, optimistic and pessimistic bounds. *Right*: Comparison of the base relative permeabilities for the 4 different saturation bins calculated along the trend lines as indicated in Figures 13-16.

CONCLUSION

- Parameterizing of flow properties enables simpler use of large sets of SCAL data when defining saturation functions for full-field applications
- Honouring wettability and physics of flow through porous media enables the construction of trend models of end points and shape parameters of relative permeability.
- The trend models are used to create wettability consistent flow properties for full-field simulations

- Admitting the general scatter of SCAL data, the trend models and *LET* correlation guides and defines smooth curves for full-field simulation
- The SCAL model/saturation functions are generated as a base case with optimistic and pessimistic bounds allowing proper evaluation and uncertainty analysis of recoverable reserves for specific fields.

ACKNOWLEDGEMENTS

We acknowledge Jon Knut Ringen and Egil Boye Petersen Jr. for valuable discussions. Statoil is acknowledged for giving permission to publish.

NOMENCLATURE

k_{ro}	= oil relative permeability	k_{rw}^0	= water relative permeability at S_{orw}
k_{rw}	= water relative permeability	X_o	= parameter in k_{ro} X = L,E,T
S_{wi}	= initial water saturation	X_w	= parameter in k_{rw} X = L,E,T
S_{wir}	=irreducible water saturation	X_{orw}	= parameter in S_{orw} X = L,E,T,M,A,B
S_{orw}	= residual oil saturation	X_{wko}	= parameter in k_{rw}^0 X = L,E,T,A,C
k_{ro}^0	= oil relative permeability at S_{wir}		

REFERENCES

1. Muskat, M., et al., *Production engineering research - Flow of gas-liquid mixtures through sands*. Transactions of the American Institute of Mining and Metallurgical Engineers. **123**: p. 69-96, 1937.
2. Guo, G., et al., *Rock Typing as an Effective Tool for Permeability and Water-Saturation Modeling: A Case Study in a Clastic Reservoir in the Oriente Basin*, in *SPE Annual Technical Conference and Exhibition*. SPE97033, Society of Petroleum Engineers: Dallas, Texas, USA, 2005.
3. Hamon, G., *Two-Phase Flow Rock-Typing: Another Perspective*, in *SPE Annual Technical Conference and Exhibition*, SPE84038, Society of Petroleum Engineers: Denver, Colorado, USA, 2003.
4. Hamon, G., *Field-Wide Variations of Wettability*, SPE63144, in *SPE Annual Technical Conference and Exhibition* Society of Petroleum Engineers Inc.: Dallas, Texas, 2000.
5. Ghedan, S.G., Q. Huang, and Y. Wu, *An Improved Approach for Generating Saturation Functions for Simulation Models Using Dynamic Rock Types*, SPE 160683, in *Abu Dhabi International Petroleum Conference and Exhibition*, Society of Petroleum Engineers: Abu Dhabi, UAE, 2012.
6. Ghedan, S.G., *Dynamic Rock Types for Generating Reliable and Consistent Saturation Functions for Simulation Models*, SPE 111295 in *SPE/EAGE Reservoir Characterization and Simulation Conference 2007*, Society of Petroleum Engineers: Abu Dhabi, UAE.
7. Sylte, A., E. Ebeltoft, and E.B. Petersen. *Simultaneous Determination of Relative Permeability and Capillary Pressure Using Data from Several Experiments*, SCA2004-17 in International Symposium of the Society of Core Analysts. Abu Dhabi, UAE, 2004.
8. Maas, J. and A.M. Schulte. *Computer Simulation of Special Core Analysis (SCAL) Flow Experiments Shared on the Internet*, SCA-9719, in *International Symposium of the SCA*. 1997. Calgary, Canada.
9. Sendra, *Sendra User Guide*, 2013, Weatherford.

10. Lomeland, F., E. Ebeltoft, and W.H. Thomas. *A New Versatile Relative Permeability Correlation*, SCA2005-32, in *International Symposium of the Society of Core Analysts*. 2005. Toronto, Canada.
11. Morrow, N.R. and N. Mungan, *Wettability and Capillarity in Porous Media*. 1971, Petroleum Recovery Research Inst. Calgary.
12. Jadhunandan, P.P. and N.R. Morrow, *Effect of Wettability on Waterflood Recovery for Crude-Oil/Brine/Rock Systems*. SPE, Vol **10** 01 (p.40-46), 1995.
13. Johannesen, E.B. and A. Graue, *Systematic Investigation of Waterflood Reducing Residual Oil Saturations by Increasing Differential Pressures at Various Wettabilities*, SPE108593., SPE, Offshore Europe, 4-7 September, Aberdeen, Scotland, U.K, 2007.
14. Spiteri, E.J., et al., *A New Model of Trapping and Relative Permeability Hysteresis for All Wettability Characteristics*. SPE Journal, Vol. **13** 03 p.277-288, 2008.
15. Lorenz, P.B., E.C. Donaldson, and R.D. Thomas, *Use of Centrifugal Measurements of Wettability to Predict Oil Recovery*, Report no. 7873, U.S Bureau of Mines, Bartlesville Energy Technology Center, 1974.
16. Pentland, C.H., et al., *Measurement of Nonwetting-Phase Trapping in Sandpacks*. SPE Journal, Vol. **15**, 02 p. 274-281, 2010.
17. Land, C.S., *Comparison of Calculated with Experimental Imbibition Relative Permeability*. SPEJ, Vol. **11**, 04 p. 419-425, 1971.
18. Lomeland, F., et al., *A Versatile Representation of Upscaled Relative Permeability for Field Applications*, SPE154487, SPE Europec/EAGE Annual Conference, 4-7 June, Copenhagen, Denmark, 2012.
19. Anderson, W.G., *Wettability Literature Survey Part 5: The Effects of Wettability on Relative Permeability*. Journal of Petroleum Technology, **39**(11): p. 1453-1468,1987.
20. Craig Jr., F.F., *The Reservoir Engineering Aspects of Waterflooding*. SPE Monograph Series. Vol. **3**. 1993: Society of Petroleum Engineers.
21. Anderson, W.G., *Wettability Literature Survey- Part 1: Rock/Oil/Brine Interactions and the Effects of Core Handling on Wettability*. Journal of Petroleum Technology, **38**(10): p. 1125-1144, 1986.
22. Buckley, J.S., K. Takamura, and N.R. Morrow, *Influence of Electrical Surface Charges on the Wetting Properties of Crude Oils*. 1989. SPE, Vol.4 03, p. 332-340, 1989.
23. Buckley, J.S., C. Bousseau, and Y. Liu, *Wetting Alteration by Brine and Crude Oil: From Contact Angles to Cores*., SPEJ Vol.1 03 p.341-350, 1996.
24. Yu, L. and J.S. Buckley, *Evolution of Wetting Alteration by Adsorption From Crude Oil*. 1997. SPE Formation Evaluation, Vol.12 01, p. 5-12
25. Buckley, J.S. and Y. Liu, *Some mechanisms of crude oil/brine/solid interactions*. Journal of Petroleum Science and Engineering, 1998. **20**(3-4): p. 155-160.
26. Buckley, J.S., Y. Liu, and S. Monsterleet, *Mechanisms of Wetting Alteration by Crude Oils*. 1998. SPEJ, Vol. **3** 01 p.54-61,1998.
27. Loahardjo, N., et al., *Oil Recovery by Sequential Waterflooding: the Effects of Aging at Residual Oil and Initial Water Saturation*, SPE154202, in *SPE Improved Oil Recovery Symposium*. 2012, Society of Petroleum Engineers: Tulsa, Oklahoma, USA.
28. Schlumberger, ECLIPSE Technical Description, Version 2013.2. 1 ed. Vol. 1, p. 975-996.